Supporting Information

Polymorph-Selective Preparation and Structural Characterization of Perylene Single Crystals

André Pick,[†] Michael Klues,[†] Andre Rinn,[†] Klaus Harms,[‡] Sangam Chatterjee,[†,§] and Gregor Witte*[,†,§]

[†] *Faculty of Physics, Philipps-Universität Marburg, D-35032 Marburg, Germany*
[‡] *Faculty of Chemistry, Philipps-Universität Marburg, D-35032 Marburg, Germany*
[§] *Material Sciences Center, Philipps-Universität Marburg, D-35032 Marburg, Germany*

Contents:

I. The crystal structures of perylene

The two polymorphs of perylene, which are denoted as α- and β-phases, are both of monoclinic type. The crystal structures are shown in Fig. S1, where in a) and c) the unit cells of the α- and β-phases are sketched. The α-phase contains four molecules per unit cell, which are arranged in a sandwich herringbone motif (cf. Fig. S1 b)), while the β-polymorph contains two molecules per unit cell that are arranged in a γ-type motif (cf. Fig. S1 d)).

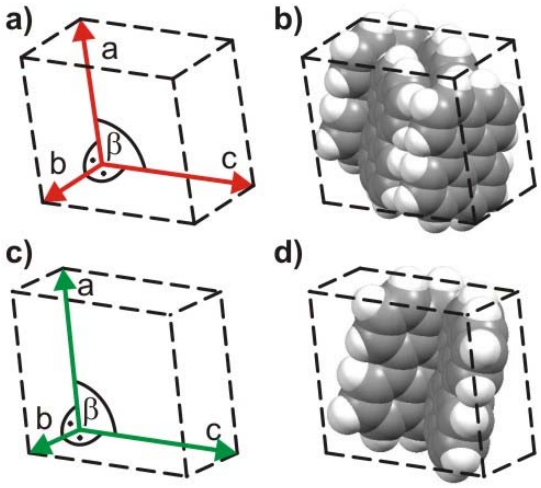

Figure S1: Unit cell and molecular packing motifs of perylene crystals in (a,b) the α-phase and (c,d) the β-phase.

	α-phase	β-phase
Z	4	2
a	10.24 Å	9.76 Å
b	10.79 Å	5.84 Å
c	11.13 Å	10.61 Å
α	90°	90°
β	100.92°	96.77°
γ	90°	90°
V/Z	301.8 $Å^3$	300.5 $Å^3$

Table S1: Unit cell parameters of both perylene polymorphs reported in [23].

To verify the presence of the known polymorphs and to enable a clear correlation with their crystallographic shape, the unit cells of perylene crystals of both phases grown from toluene solution were also determined in this study at 100K. As presented in Tab. S2 they are in excellent agreement with the literature data [23] listed in Tab. S1 that were taken at 150K (α-phase) and 200K (β-phase).

	α-phase	β-phase
a	10.21 Å	9.77 Å
b	10.77 Å	5.82 Å
c	11.06 Å	10.55 Å
α	90°	90°
β	101.13°	96.92°
γ	90°	90°

Table S2: Unit cell parameters determined in this study for solution grown perylene crystals.

Crystals of the α-phase are known to be stable up to their melting point, while the β-phase irreversibly transforms into the α-phase at about 373K [23]. In Fig. S2 single-crystals of perylene are shown, which were prepared by re-sublimation between two substrates. Here, the sample was heated within 30 min from 300K to 400K. Postdeposition heating at ambient conditions confirms, that the β-phase is thermically less stable, as the crystal in b) is nearly sublimed at 165°C, while the α-phase appears stable, apart from some changes in reflectivity.

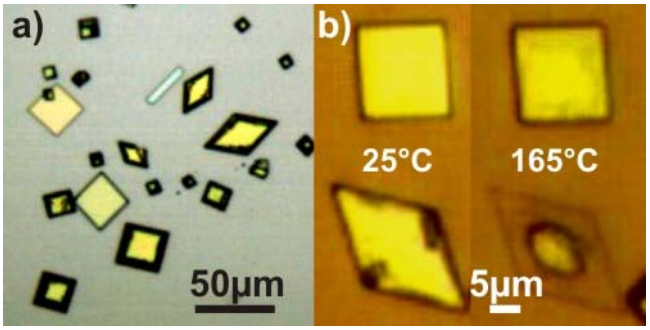

Figure S2: (a) Single crystals of α- and β- perylene observed upon re-sublimation. (b) Comparison of the thermal stability of crystallites of both polymoprhs upon heating at ambient conditions, indicating a lower thermal stability of the β- polymorph (lower row).

Apart from the two known polymorphs, we observed also an interface mediated thin film phase (cf. Fig. 4). It especially occurs when depositing perylene by OMBD on an oxidized Si-wafer, while an increasing number of cycles of re-sublimation between two substrates leads to a increasing α-phase-signal. The diffractogram in Fig. 4 d) has been obtained for a sample, which is presented in Fig. S3, where also pyramidal crystallites of the β-phase are present.

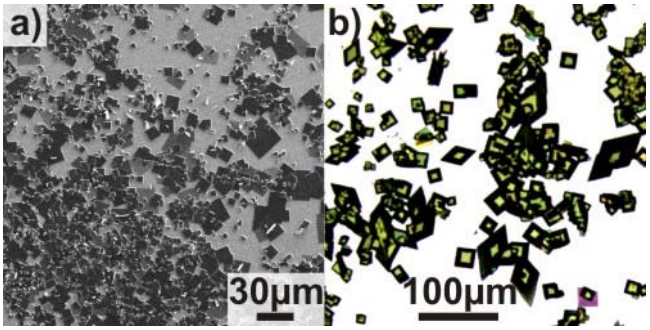

Figure S3: (a) SEM micrograph of accumulated α-crystals and (b) optical migrograph of preferentially formed pyramidal crystallites of the β-phase on the same sample. Re-sublimation was performed by applying a heating ramp from 300K to 385K within 1h.

For polarization resolved spectroscopic studies it is crucial to know the exact azimuthal orientations within the (100) top-faces. Therefore, in-plane measurements were performed to identify specific azimuth directions and thus the relative orientation of unit cell vectors with respect to the characteristic shape of the crystallites. For this purpose the (011) reflex was used which was obtained by tilting the sample at the angles ω and ψ for the α- and β-phase respectively (angles between (100) and {011} planes) such that the Bragg-reflex of the (011) planes was observed and subsequently rotating the samples around the a* axis as shown schematically in Fig. S4. Here, the

exact orientation of the single-crystals is crucial: the (0-11) reflex is thus calibrated to 0°. Although opposing planes are parallel, only one reflex appears. This is due to the monoclinic nature of both crystal structures: As the sample rotates, e.g. the (011) plane encloses a cone, so that there is only one position for a reflex. Altogether we obtain two reflexes, the second one belongs to the (0-11) or the (01-1) plane. Those enclose angles, which correspond to the angles σ and τ, which are those when looking ontop of the (100) plane of a crystal.

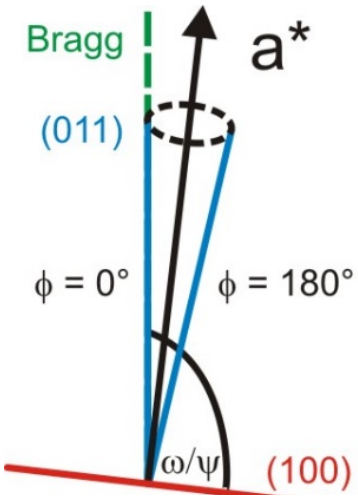

Figure S4: Scheme for the in-plane scan geometry.

In summary, the {011} planes are indeed the occuring side faces of the single-crystals, which is visualized in Fig. S5 where top views of such planes are shown for both phases.

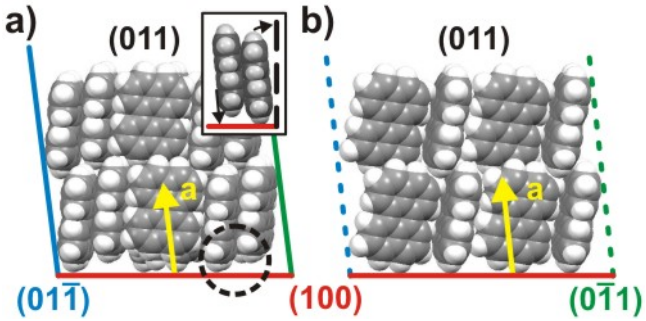

Figure S5: Top views of the (011) planes together with the belonging molecular packing motifs of both polymorphs of perylene. (a) For the α-phase the (01-1) (blue) and (0-11) (green) side faces are oriented nearly perpendicular (angle σ=92°) with respect to the drawing plane, while for the β-phase they form an angle of τ=122°. Therefore, the projection of the side faces are shown as dashed lines in (b). The inset in (a) explains the formation of a thin-film-phase: one of the sandwiched molecules in the α-phase is vertically slightly shifted, so that only every second molecule is in contact with a supporting substrate. By contrast in the substrate-mediated thin film phase the (100)-interlayer spacing is somewhat increased. This can be attributed to a levelling of all molecules within the layer which enables contact with the substrate and in turn causes a more upright tilting of the molecules.

II. Morphological characteristics of single-crystals and thin-films

Truncated pyramidal single-crystals were obtained upon repeated re-sublimation, which exhibit screw-dislocations on top of their surfaces as shown in Fig. 5. We note further that the side faces of such pyramids can not be attributed to low-indexed planes. Instead they exhibit characteristic kinks, which are also seen in the confocal laser scanning fluorescence micrographs in Fig. 10, and indicate the presence of stacked slices forming an overal pyramidal shape. This can be clearly seen in the atomic force micrographs shown in Fig. S6, where a pyramidal crystal is shown in a 3D presentation together with belonging topographic line scans and a derivative image to emphasize the kinks.

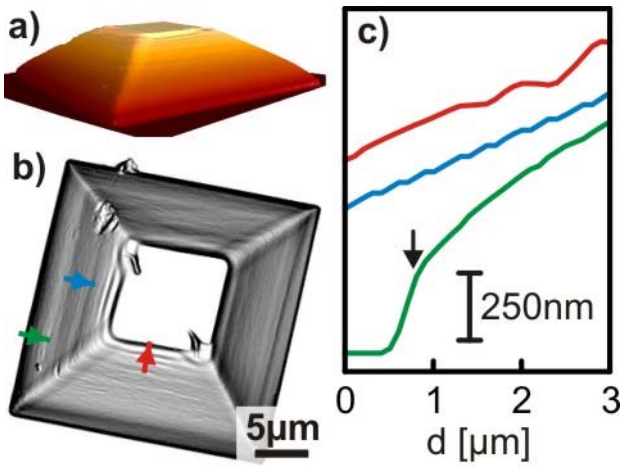

Figure S6: AFM data of a pyramidal grown α-phase single-crystal obtained from re-sublimation: (a) 3D topography, (b) derivative of the topography, emphasising the presence of kinks, which are also shown in the appropriate topographical cross sections in (c).

The presence of screw-dislocations on crystals prepared upon re-sublimation can be interpreted in terms of a kinetically driven process, where strain is released. This is further evidenced when comparing films which were prepared by rather different growth rates using a rapid and a slow re-sublimation process. Fig. S7 shows belonging AFM micrographs for different temperature ramps upon re-sublimation, revealing a spiral growth-mode only for the case of of a high sublimation rate.

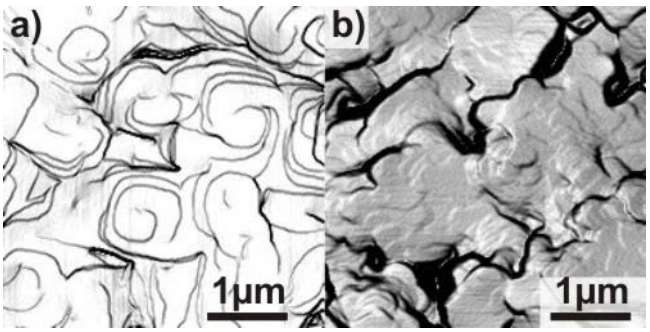

Figure S7: comparison of AFM micrographs of perylene films prepared by re-sublimation of powder between two substrates for different heating ramps: (a) from 300K to 400K in less than 2min. yielding a pronounced spiral growth, (b) from 300K to 390K in 1h, showing no screw-dislocations. For better visualization the images are shown as derivative to enhance the step edges.

In contrast to the pyramidal crystallites, we observed impressively flat surfaces for platelet crystallites upon re-sublimation. Platelet shaped perylene crystallites were also obtained by liquid-mediated growth which appear rather homogeneous in the optical microghraphs (cf. next section). Unfortunately, AFM measurements of such samples are largely hampered by the oil film which coveres the crystallites. Attempts to still perform tapping mode AFM measurements were not successful as the crystallites are not fixated and move in the liquid. However, we observed a slow but notable dewetting of the oil from the crystallites. Several months after preparation the oil was withdrawn from the crystals so that morphological measurements become possible. Fig. S8 shows an optical micrograph of an α-crystal 10 months after its preparation in oil together with AFM data confirming that platelet crystals grown in oil have a similar thickness and flatness compared to platelets obtained from re-sublimation. Note, that some arears of the oil remain on the surface appearing as spikes in the line scan (blue line in panel c).

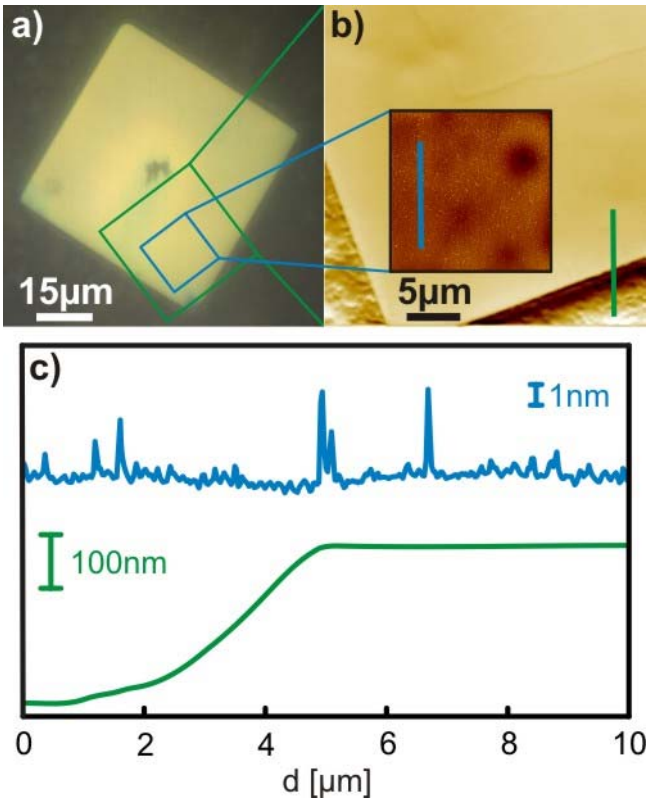

Figure S8: (a) Optical micrograph of an α-phase perylene crystal prepared by liquid-mediated growth recorded several month after its preparation together with (b,c) corresponding AFM data which is made possible by an extensive dewetting and shows the presence of a remarkable flatness of the platelet crystallite.

III. Preparation of single-crystals by liquid-mediated growth

Growth of perylene layers by OMBD into thin films of silicone-oil reveals similarity to the growth from solution. In particular the supersaturation of the oil is demonstrated by mechanically scratching a film, where perylene has been deposited into, but no nucleation has taken place. As can be seen in Fig. S9, small but distinct crystallites spontaneously nucleate during the scratching, hence reflecting a supersaturation of the film.

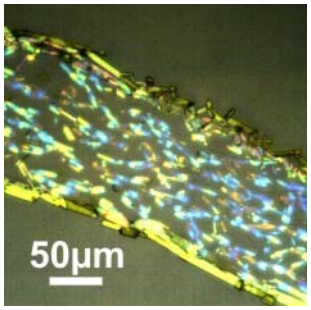

Figure S9: Instantaneously nucleating crystallites induced by scratching a silicone-oil film directly after perylene-deposition, indicating that the oil is in a supersaturated state during deposition.

By tuning the deposition conditions, we were able to prepare large single-crystals of both polymorphs. However, at some point the crystals do not become larger in their lateral dimensions, as small crystallites start to nucleate. This can be seen in Fig. S10, where the nominal thickness, as well as the molecular flux were slightly increased compared to Fig. 9 a).

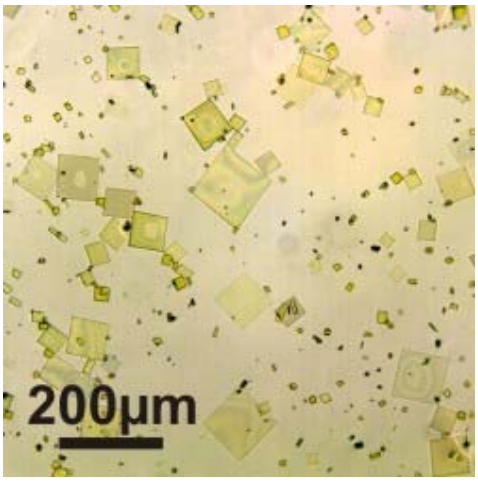

Figure S10: Optical micrograph showing a competing formation of small perylene crystallites in addition to the ripening of existing platelet shaped crystals (growth parameters T_S =310K, R=8Å/min and d_{nom} =80nm).

β-phase crystallites have been obtained for two different growth parameter regimes. The first one is characterized by a very low deposition rate of 1-2 Å/min and a substrate temperature of 290K which is lower than for the preparation of α-phase crystals (cf. Fig. 9 b). However, when increasing the substrate temperature to 325K and the deposition rate to 30-60Å/min also a formation of crystallites of both polymorphs was found. Fig. S11 shows some optical micrographs of this scenario. In a) an overview is given, showing in particular a frequent twinning of α-crystals together with some β-crystals, while in b) an individual β-crystal is shown, which is tilted slightly, as can be seen from the differently focused edges. This tilting of (100)-planes leads to reduced x-ray diffraction peak

intensities in belonging out-of-plane XRD measurement (cf. Fig. 9). In panel c) further crystals are shown, where again we find twinning at the edges of β-crystals and distorted α-crystals. Panel d) depicts a hexagonally shaped crystal, which can be understood as a truncated β-crystal by introducing additional side faces as already reported in [34].

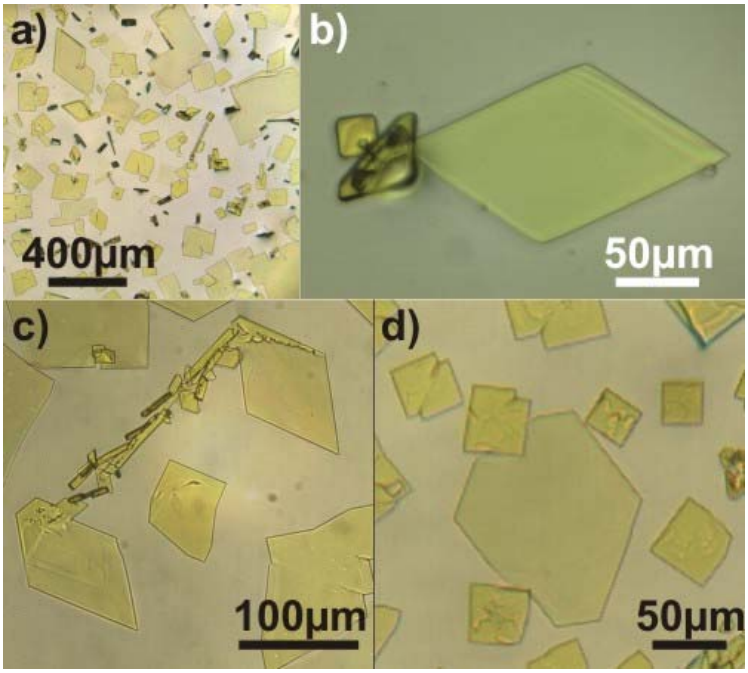

Figure S11: Summary of optical micrographs of perylene crystallites obtained by liquid-mediated growth at elevated substrate temperatures: (a) Mixture of both phases for nominal 630nm at 325K and 30Å/min. (b) Slightly tilted β-crystal grown at 325K and 50Å/min. (c) twinned β-phase crystals together with distorted α-phase crystals grown at 910nm at 325K and 60Å/min, (d) A hexagonal shaped β-crystal grown at the same conditions as given in (c).

When increasing the rate of deposition further, a pronounced needle growth occurs, which is similar to the scenario observed in [53]. Corresponding fluorescence micrographs (cf. Fig. S12b) and next section) show that these needles exclusively adopt the α-phase. However, the skeletal characteristics are less pronounced in our case, as an elevated substrate temperature of 325K was used instead of room temperature used in [53]. We note that remaining silicon oil droplets with dissolved perylene cause parasitical green fluorescence as depicted in Fig. S12c).

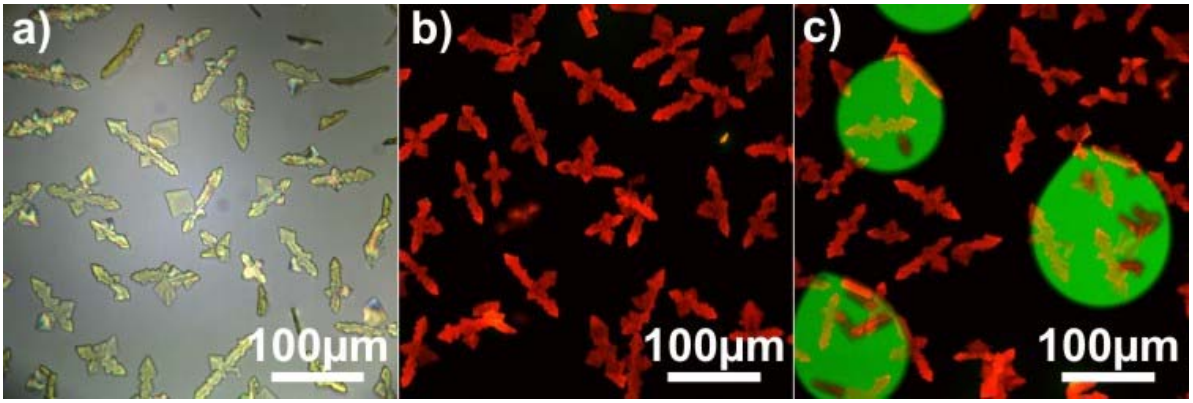

Figure S12: (a) Needle-like growth of perylene in silicone-oil together with (b) CLSF-micrograph confirming that the skeletal crystals are grown in the α-phase (deposition parameters: 80nm grown at 325K, rate 800Å/min), while perylene dissolved in remaining silicone oil causes green fluorescence (c).

IV. Optical characterization

Single-crystals have been characterized by means of CLSFM, which is a very useful tool to distinguish the two phases of perylene because of their different fluorescence.

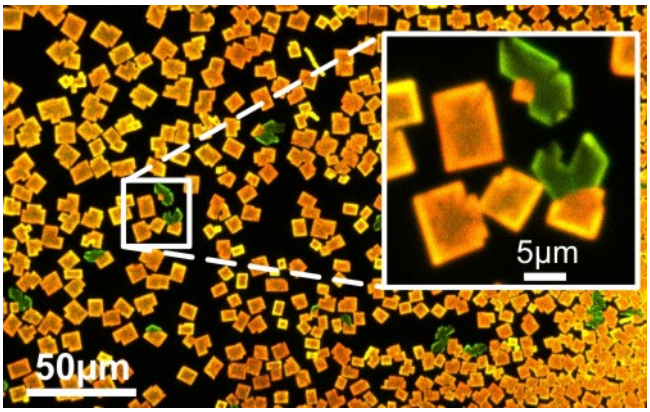

Figure S13: Fluorescence micrograph of α- and β-perylene prepared by re-sublimation showing a majority of α-perylene crystals.

We want to emphasize that photoluminescence spectra can differ, if measuring at different positions of a crystal. Fig. S14 compares fluorescence spectra that were recorded in the middle and at the edge or corners of perylene crystals. It can be seen that, additional signals appear, when integrating the intensities right at the edges or corners, which should be taken into account when recording the PL. This fact can be related to a wave-guide effect, as the edges and steps are emitting significantly more intensity than the centre of a crystal as discussed in the main paper.

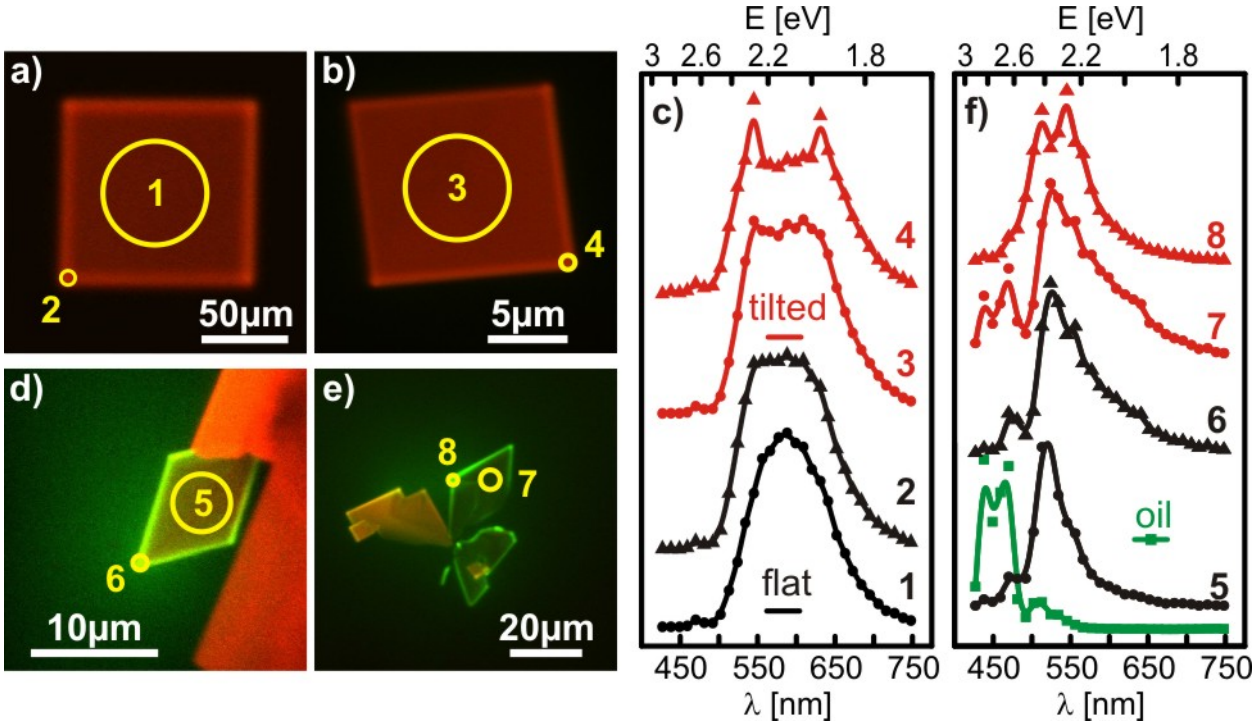

Figure S14: CLFS-micrographs of α-phase (a,b) and β-phase perylene crystals (d,e) together with corresponding spatially resolved fluorescence spectra (c,f) showing characteristic differences for emission at the center, edges or corners of the crystallites.

Furthermore it should be noted that the spectra in Figure S14 have been recorded by a commercially available CLSFM system. Despite its obvious ease-of-use such systems offer, they have several downsides. One should carefully check if the standard settings interpolate the measured data by a spline mimicking smooth curves. Also, the spectral response may not be calibrated against traceable sources. For this purpose, additional fluorescence spectra have been recorded at the center of platelet perylene crystals using a specific photoluminescence setup which had been carefully calibrated by considering the spectral response of the detector. As shown in Figure S15 this affects the spectral shape considerably. We note that the uncorrected spectra much closer resemble published fluorescence spectra (see, e.g. ref.[28,33]), thus indicating that the spectral response of the detector may have not been considered properly.

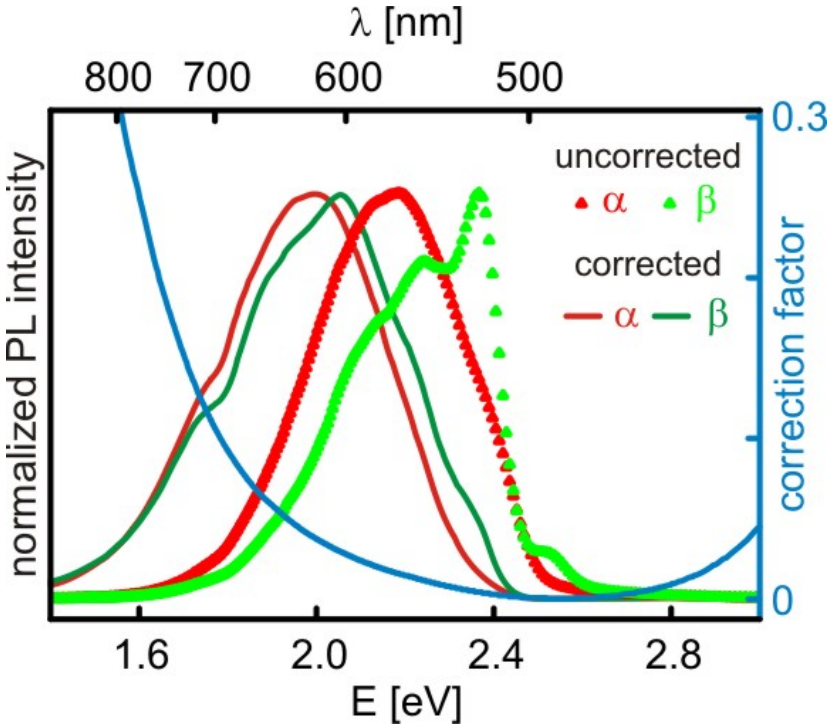

Figure S15: Normalized corrected spectra (solid lines) and uncorrected, as measured photoluminescence data (dotted) of the perylene α- (red) and β- (green) phases. The correction factor is shown in blue for the relevant spectral range.